Tight-binding treatment of the Hubbard model in infinite dimensions

L. Craco
Instituto de Física, Universidade Federal do Rio Grande do Sul, 91501-970 Porto Alegre, Rio Grande do Sul, Brazil

M. A. Gusmão*
Laboratoire de Physique Quantique, Université Paul Sabatier, CNRS (URA 505), 118 route de Narbonne, 31062 Toulouse, France
(Received 16 February 1996)

We discuss the infinite dimension limit of the Hubbard model by means of a perturbative expansion of the one-particle Green's function around the atomic limit. The diagrammatic structure is simplified in this limit, allowing a formal resummation that reproduces a previously proposed mapping to a single-site mean-field problem. The method provides a natural way of addressing this effective problem by means of a perturbative expansion in the local mean field. This gives the correct exact result for the Falicov-Kimball model, which is used as a starting point to study the Hubbard case. [S0163-1829(96)04727-3]

I. INTRODUCTION

The limit of infinite spatial dimensionality introduced by Metzner and Vollhardt[1] has been very useful in understanding strongly correlated fermion systems. In this limit, the Hubbard model[2] can be exactly mapped into a single-site problem in the presence of an effective field that describes its connection to the rest of the lattice.[3] In contrast to localized spin models, for which the mean-field solution is exact in infinite dimensions, an exact solution of the fermionic effective problem has not yet been found, except[4,5] for the Falicov-Kimball (FK) model,[6] that can be viewed as a simplified version of the problem. The full Hubbard model has been addressed by numerical methods[7–10] or a combination of those and weak-coupling perturbation theory.[11,12] An alternative approach, based on a (strong-coupling) perturbation expansion of the one-particle Green's function around the atomic limit is discussed here. Within this approach, the structure of the diagrammatic representation of the perturbation series is greatly simplified in the infinite dimension limit. From a formal point of view, one easily recovers the mapping to a single-site effective problem. In the case of the FK model, the resulting equations can be completely solved to give the exact site-diagonal single-particle Green's function $G_{ii}(i\omega_n)$, reproducing a solution previously obtained by Brandt and Mielsch.[4] We then use this as a starting point for the study of the complete Hubbard model, constructing approximate solutions by adding corrections to the Green's function of the FK model.

In this paper, we discuss the general ideas behind this method, and exemplify their applicability by constructing a simple approximate solution of the Hubbard model in infinite dimensions. For the paramagnetic case this approximation, besides reproducing correctly the expected behavior of the single-particle density of states (DOS) in the large-U limit, yields a three-peaked DOS for small U, in agreement with weak-coupling and numerical calculations, although deviations from Fermi-liquid behavior are still observed. As far as the physically more relevant antiferromagnetic (AF) state is concerned, our simple approximation reveals a strong memory of the FK limit from which it is derived, and the spin symmetry of the Hubbard model is not completely recovered. The phase diagram that we obtain differs from that obtained by numerical methods,[7,12] in that the critical temperatures are always smaller than those of the FK model for the same values of U. Indeed, we argue that this is what should actually be expected on physical grounds.

II. PERTURBATIVE CALCULATION

We consider the Hubbard model with nearest-neighbor hopping on a d-dimensional hypercubic lattice,[13] which is described by the Hamiltonian

$$H=-\mu\sum_{i\sigma} n_{i\sigma}+U\sum_{i} n_{i\uparrow}n_{i\downarrow}-t\sum_{\langle ij\rangle\sigma} c^{\dagger}_{i\sigma}c_{j\sigma}, \qquad (1)$$

in the usual notation. The first two terms on the right hand side of Eq. (1) will be considered as the unperturbed Hamiltonian, while the last one will be taken as the perturbation. We will be interested in the temperature dependent one-particle Green's function,

$$G_{ij\sigma}(\tau)\equiv-\langle \hat{T}c_{i\sigma}(\tau)c^{\dagger}_{j\sigma}(0)\rangle. \qquad (2)$$

A diagrammatic representation of the perturbation series for this function has been introduced by Metzner.[14] After Fourier transforming in space and imaginary time, we can write a Dyson-like equation[15]

$$G_{\mathbf{k}\sigma}(i\omega_n)=\mathcal{G}_{\mathbf{k}\sigma}(i\omega_n)+\mathcal{G}_{\mathbf{k}\sigma}(i\omega_n)\varepsilon_{\mathbf{k}}G_{\mathbf{k}\sigma}(i\omega_n), \qquad (3)$$

where $\omega_n\equiv(2n+1)\pi T$ (integer n) is a fermionic Matsubara frequency, $\varepsilon_{\mathbf{k}}$ is the Fourier transform of the hopping term, and $\mathcal{G}_{\mathbf{k}\sigma}(i\omega_n)$ is the *irreducible part* of the one-particle Green's function.[15] We can, then, formally write

$$G_{\mathbf{k}\sigma}(i\omega_n)=\frac{1}{[\mathcal{G}_{\mathbf{k}\sigma}(i\omega_n)]^{-1}-\varepsilon_{\mathbf{k}}}. \qquad (4)$$

The irreducible Green's function $\mathcal{G}_{\mathbf{k}\sigma}(i\omega_n)$ has a diagrammatic representation[15] in which the vertices are associated with cumulant averages of electron creation and annihilation operators at the same site. These diagrams are *irreducible* in

the sense that they cannot be separated in two disconnected parts by the process of cutting a single hopping line. The explicitly *local* diagrams of this function, i. e., those with a single external vertex, can also be interpreted as the diagrammatic representation of the site-diagonal Green's function $G_{ii\sigma}(i\omega_n)$, with an important difference: in the cumulant average associated with the external vertex, we have to take into account only the terms in which the two external operators appear in the same average. Equivalently, the external vertex can be considered as a simple (noncumulant) local average, and the sum over internal sites must *not* include the one corresponding to the external vertex. The local averages can be calculated by rewriting the fermion operators in terms of Hubbard operators,[16,17] and introducing an intravertex diagrammatics.[15] This provides, in principle, a direct way of calculating the complete local Green's function. On the other hand, combining Eq. (4) the identity $G_{ii\sigma}(i\omega_n) \equiv (1/N)\Sigma_{\mathbf{k}} G_{\mathbf{k}\sigma}(i\omega_n)$, and we can write

$$G_{ii\sigma}(i\omega_n)=\frac{1}{N}\sum_{\mathbf{k}}\frac{1}{[\mathcal{G}_{\mathbf{k}\sigma}(i\omega_n)]^{-1}-\varepsilon_{\mathbf{k}}}. \tag{5}$$

If one calculates directly $G_{ii\sigma}(i\omega_n)$ as commented above, Eq. (5) can be viewed as a self-consistency condition to be fulfilled. This is a key point in the general strategy of performing renormalizations of the local Green's function, and will be particularly useful in the analysis of the infinite dimension limit, as we will see in the next sections.

III. THE INFINITE DIMENSION LIMIT

When generalizing the Hubbard model to a lattice of infinite dimensionality one has to choose an appropriate scaling of the hopping amplitudes in order to preserve a finite energy per particle. This scaling has been proven[1] to be $dt^2=$ const. Each unconstrained sum over internal sites in a diagram gives a factor of order d (in hypercubic lattices the coordination number is $z=2d$). However, topological constraints of the diagrams may severely reduce this multiplicity. The case of a simple loop with $2p$ hopping steps is easy to analyze: one can roughly consider that there is free choice of each step in the first half of the *walk*, yielding a factor d^p, while the multiplicity factor of the second half is of an order of one to match the constraint of returning to the initial site with the remaining p steps. The factor d^p coming from the summation over internal sites exactly compensates the factor $(1/\sqrt{d})^{2p}$ associated with the hopping amplitudes, and the simple loops are of $O(d^0)$. With this kind of reasoning it is possible to show that only the site-diagonal part of the irreducible Green's function $\mathcal{G}_\sigma(i\omega_n)\equiv(1/N)\Sigma_{\mathbf{k}}\mathcal{G}_{\mathbf{k}\sigma}(i\omega_n)$ survives in the limit $d=\infty$, and only diagrams with independent loops are nonvanishing.

From the above discussion, we can conclude that the general structure of the diagrams contributing to $G_{ii\sigma}(i\omega_n)$ is that depicted in Fig. 1. All the lines that go in and out of the external vertex are identical, and represent the quantity

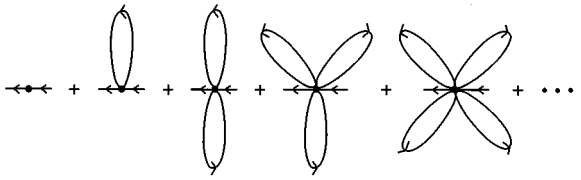

FIG. 1. Diagrammatic series representing the site-diagonal Green's function $G_{ii\sigma}$ in $d=\infty$.

$$\mathcal{A}_\sigma(i\omega_m)\equiv{\sum_l}' t_{il}\mathcal{G}_\sigma(i\omega_m)t_{li} + {\sum_{ll'}}' t_{il}\mathcal{G}_\sigma(i\omega_m)t_{ll'}\mathcal{G}_\sigma(i\omega_m)t_{l'i}+\ldots, \tag{6}$$

where the sums are restricted to sites other than i to avoid having a cumulant average on this site. It is straightforward to show that[15]

$$\mathcal{A}_\sigma(i\omega_m)=\frac{\tilde{\mathcal{A}}_\sigma(i\omega_m)}{1+\tilde{\mathcal{A}}_\sigma(i\omega_m)\mathcal{G}_\sigma(i\omega_m)}, \tag{7}$$

where

$$\tilde{\mathcal{A}}_\sigma(i\omega_m)=\frac{1}{N}\sum_{\mathbf{k}}\varepsilon_{\mathbf{k}}^2 G_{\mathbf{k}\sigma}(i\omega_m). \tag{8}$$

Thus,

$$\mathcal{A}_\sigma=\mathcal{G}_\sigma^{-1}-G_{ii\sigma}^{-1}. \tag{9}$$

If we use this equation to eliminate $\mathcal{G}_\sigma$, Eq. (5) can be written as

$$G_{ii\sigma}=\frac{1}{N}\sum_{\mathbf{k}}\frac{1}{G_{ii\sigma}^{-1}+\mathcal{A}_\sigma-\varepsilon_{\mathbf{k}}}. \tag{10}$$

Since the $\mathbf{k}$ dependence is restricted to the tight-binding energies $\varepsilon_{\mathbf{k}}$, we can replace the sum over $\mathbf{k}$ by an integral in energy in the form

$$G_{ii\sigma}=\int d\varepsilon\frac{\rho_0(\varepsilon)}{G_{ii\sigma}^{-1}+\mathcal{A}_\sigma-\varepsilon}\equiv F(G_{ii\sigma}^{-1}+\mathcal{A}_\sigma), \tag{11}$$

where $\rho_0(\varepsilon)$ is the uncorrelated density of states in $d=\infty$. For a hypercubic lattice, and choosing $4dt^2\equiv t^{*2}=1$, $\rho_0(\varepsilon)=(1/\sqrt{\pi})\exp(-\varepsilon^2)$.[1] With this choice, from now on all the energies will be expressed in units of t^*.

From the diagrams of Fig. 1, we can see that $\mathcal{A}_\sigma$ describes the motion of an electron through the *surrounding medium* of site i, i.e., the rest of the lattice. Its effect can be viewed as equivalent to that of a time-dependent *field* coupling the lattice site i to a reservoir of particles (or rather two reservoirs, one for each spin species). Thus, the problem has been reduced to an effective *single-site* Hubbard model in the presence of the fields $\mathcal{A}_\sigma$, and subject to the self-consistency condition (11). The single-site problem can be thought of as being described by the effective action[3]

$$\mathcal{S}=\mathcal{S}_{\mathcal{A}}^0+U\int_0^\beta d\tau\, n_\uparrow(\tau)n_\downarrow(\tau), \tag{12}$$

where $\mathcal{S}^0_{\mathcal{A}}$, the action for noninteracting electrons in the presence of an effective field $\mathcal{A}$, is given by

$$\mathcal{S}^0_{\mathcal{A}} = -\int_0^\beta d\tau \int_0^\beta d\tau' \sum_\sigma c^\dagger_\sigma(\tau)\hat{G}^{-1}_\sigma(\tau-\tau')c_\sigma(\tau'), \tag{13}$$

with

$$\hat{G}^{-1}_\sigma(\tau-\tau') \equiv (\partial_\tau+\mu)\delta(\tau-\tau') - \mathcal{A}_\sigma(\tau-\tau'). \tag{14}$$

The method of perturbation around the atomic limit not only reproduces the exact mapping of the infinite dimensional problem to a single-site effective one, but also provides a natural way of analyzing this effective problem by means of an expansion in powers of the fields $\mathcal{A}_\sigma$. This point will be further explored in what follows.

IV. PERTURBATION APPROACH TO THE SINGLE-SITE PROBLEM

As mentioned before, our method yields an approach for solving the single-site effective problem (12–14) as a perturbation series in the fields $\mathcal{A}_\sigma$ (see Fig. 1). Starting with the unperturbed local Green's function $-\langle \hat{T} c_\sigma(\tau) c^\dagger_\sigma(0)\rangle_0$, each order in perturbation theory introduces a product of the type $\mathcal{A}_{\sigma_1}(\tau_1-\tau_1')c^\dagger_{\sigma_1}(\tau_1)c_{\sigma_1}(\tau_1')$, so that, in general, one has to calculate averages of the form $\langle c^\dagger_{\sigma_1}(\tau_1)c_{\sigma_1}(\tau_1')c^\dagger_{\sigma_2}(\tau_2)c_{\sigma_2}(\tau_2')\cdots\rangle_0$. For this we use the representation $c_\sigma = X_{0\sigma} + \sigma X_{\bar{\sigma}2}$, where the Hubbard operators[16] are defined as $X_{\alpha\beta} \equiv |\alpha\rangle\langle\beta|$, in the basis of the four eigenvectors representing an empty site ($|0\rangle$), a singly occupied site with both possible spin orientations ($|\sigma\rangle = |\uparrow\rangle$ or $|\downarrow\rangle$), and a doubly occupied site ($|2\rangle$). In its initial form, each average involves only the ''fermionic'' Hubbard operators appearing in the representation of c_σ or $c^\dagger_\sigma$. The direct *contraction* (in the sense of Wick's theorem[18]) between the two external operators must be excluded, since it is automatically taken into account by the renormalization of the average number of electrons in the atomic Green's function.[15] When all operators correspond to the same spin (say, σ) contractions can only generate the opposite-spin projectors $n_{\bar{\sigma}}$ or $1-n_{\bar{\sigma}}$, which act as c numbers with respect to the remaining operators. Thus, the whole process is exactly the same as in usual many-body treatments, except for a final average value of the relevant projector. This allows for the exact solution of a simplified version of the model, as we discuss next.

A. The Falicov-Kimball model

Although originally proposed in a different context,[6] the Falicov-Kimball model can be viewed as a simplified Hubbard model in which only electrons with a given spin orientation (say, spin-up) can hop through the lattice. The other electrons (spin-down) have frozen dynamics. However, they are thermodynamically coupled to the moving electrons, and their number per lattice site is not *a priori* fixed. The entire analysis developed for the Hubbard model holds here, but the single-site effective problem is simplified by the fact that only electron operators with the same spin index appear in the local averages. Thus, the general structure of the intravertex diagrams is as shown in Fig. 2. The dashed lines represent any of the two possible contractions between the Hubbard operators that compose a fermionic one. They give rise to factors $g_\alpha(i\omega_n) = 1/(i\omega_n - \varepsilon_\alpha)$, where ε_α are the single-site one-particle excitation energies, which can be $\varepsilon_{0\uparrow} = -\mu$ and $\varepsilon_{\downarrow 2} = -\mu + U$. These factors are also multiplied by the projectors $(1-n_\downarrow)$ or $n_\downarrow$, respectively. Since the latter are orthogonal projectors, only powers of the same g_α can appear in each term. This gives two independent power series (in $g_{0\uparrow}$ and $g_{\downarrow 2}$) that can be summed up to give

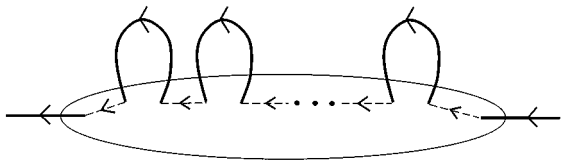

FIG. 2. Generic diagram of $G_{ii\sigma}$ for the FK model in $d=\infty$.

$$G_{ii\uparrow}(i\omega_n) = \frac{1-\langle n_\downarrow\rangle}{i\omega_n+\mu-\mathcal{A}(i\omega_n)} + \frac{\langle n_\downarrow\rangle}{i\omega_n+\mu-U-\mathcal{A}(i\omega_n)}, \tag{15}$$

where it is implicit that $\mathcal{A}(i\omega_n)$ acts only on spin-up electrons. This site-diagonal Green's function, which has the same form as obtained from the *scattering correction* term of the Hubbard III approximation for the Hubbard model,[19] reproduces the exact solution of the FK model obtained by Brandt and Mielsch.[4] They arrived at this form following an argument based on the fact that the self-energy depends on the kinetic term only through G_{ii}. Here, we have arrived at the same result by means of an exact summation of the perturbation series in the effective field $\mathcal{A}$. In the more general case of the Hubbard model, even if it remains true that the self-energy[20] is site diagonal in $d=\infty$ and depends on the kinetic term only through the local Green's functions (for both spin orientations), the latter no longer have the simple form of Eq. (15).

B. Inclusion of local spin fluctuations

We now go back to the complete Hubbard model, allowing for the hopping of electrons of both spin orientations. When operators corresponding to different spins are present, their contractions give rise to ''bosonic'' Hubbard operators of the form $X_{\bar{\sigma}\sigma}$ (spin flip of a singly occupied site) or X_{02} (annihilation of a doubly occupied site) and their Hermitian conjugates. In principle, in order to make full use of well known many-body methods, these operators should be treated in equal footing with respect to the fermionic ones. In order to eliminate the bosonic operator as soon as possible, we choose as a priority rule that contractions (in this case defined by the commutator) must be started by a bosonlike operator. In contrast, when only fermionlike operators are present in an average, we choose as a priority rule that contractions should start with an annihilation operator.[21]

There are, however, some inconveniences in using the above rules. For instance, the operator $X_{\bar{\sigma}\sigma}$ commutes with the unperturbed Hamiltonian, due to the symmetry of the Hubbard model under spin inversion. Similarly, at half filling

the particle-hole symmetry of the model causes X_{02} to commute with the unperturbed Hamiltonian too. Then, the Green's functions associated with these operators (and appearing as a result of their contractions) have the form $1/i\nu_n$, diverging when the bosonic Matsubara frequency $\nu_n \equiv 2n\pi T$ is equal to zero. A possible way to circumvent this problem is to introduce an external magnetic field to break the spin inversion symmetry, and to work at a generic filling n, which fixes the chemical potential μ. However, results at zero-field and/or for the half-filling case involve a delicate limiting process, at least one that is very difficult to achieve in a practical calculation.[15] On the other hand, a *pedestrian* approach to time-ordered averages would be to calculate the products in all possible orderings. The main disadvantage of this procedure is that it produces a multiplicity of constraints for the integrations over internal times. Here, we have chosen a mixed approach: we use contractions when only fermionlike operators are present, but work out all possible products whenever a bosonlike operator appears. In general, only a very limited number of time orderings are nonzero, which are easy to figure out due to the simple product rule for Hubbard operators ($X_{\alpha\beta}X_{\epsilon\gamma} = \delta_{\beta\epsilon}X_{\alpha\gamma}$).

We will exemplify this procedure by evaluating one of the terms contributing to the four-operator average,

$$\Gamma^{(4)}_{\sigma\bar{\sigma}}(\tau,\tau_1,\tau_2) \equiv \langle \hat{T} c_\sigma(\tau) c^\dagger_{\bar{\sigma}}(\tau_1) c_{\bar{\sigma}}(\tau_2) c^\dagger_\sigma(0)\rangle, \quad (16)$$

that appears in the one-loop diagram of Fig. 1. When we rewrite this in terms of Hubbard operators, one of the terms is

$$\Gamma_1 = \langle \hat{T} X_{0\sigma}(\tau) X_{\bar{\sigma}0}(\tau_1) X_{0\bar{\sigma}}(\tau_2) X_{\sigma 0}(0)\rangle. \quad (17)$$

After the first contractions, led by $X_{0\sigma}(\tau)$, and remembering not to take into account the direct contraction with the other external operator (at time 0), we have

$$\Gamma_1 = -g_{0\sigma}(\tau-\tau_1)\langle \hat{T} X_{\bar{\sigma}\sigma}(\tau_1) X_{0\bar{\sigma}}(\tau_2) X_{\sigma 0}(0)\rangle. \quad (18)$$

At this stage there is a bosonic operator in the average, and we have to write down explicitly all possible time-ordered products. Actually, since τ_1 and τ_2 are integrated between 0 and β, the only nonzero product is $X_{0\bar{\sigma}}(\tau_2) X_{\bar{\sigma}\sigma}(\tau_1) X_{\sigma 0}(0)$, with the constraint $\tau_2 > \tau_1 > 0$. Now we use the fact that $X_{\bar{\sigma}\sigma}$ is time independent to eliminate it by performing the product of the first two operators. This gives

$$\Gamma_1 = -g_{0\sigma}(\tau-\tau_1)\,\theta(\tau_2-\tau_1)\langle \hat{T} X_{0\sigma}(\tau_2) X_{\sigma 0}(0)\rangle, \quad (19)$$

where $\theta(\tau_2-\tau_1)$ is the step function, and again we used the fact that $\tau_2 > 0$ to reinsert the time-ordering operator in the remaining average. This allows us to write, finally,

$$\Gamma_1 = g_{0\sigma}(\tau-\tau_1)\,\theta(\tau_2-\tau_1) g_{0\sigma}(\tau_2)\langle 1-n_{\bar{\sigma}}\rangle. \quad (20)$$

Calling Λ_1 the contribution of this term to the irreducible Green's function, and leaving aside for the moment the factor $\langle 1-n_{\bar{\sigma}}\rangle$, we have

$$\Lambda_1 = \int_0^\beta d\tau_2 \int_0^{\tau_2} d\tau_1 g_{0\sigma}(\tau-\tau_1)\mathcal{A}_\sigma(\tau_1-\tau_2) g_{0\sigma}(\tau_2). \quad (21)$$

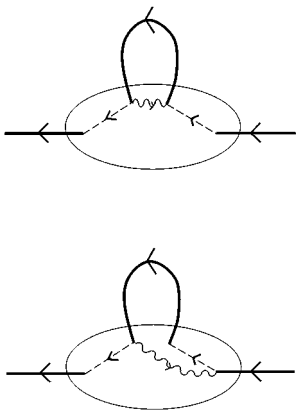

FIG. 3. Diagrammatic representation of $\Lambda^1(i\omega_n)$ (see text).

Fourier transforming Λ_1, we can write

$$\Lambda_1(i\omega_n) = \frac{1}{\beta^2} g_{0\sigma}(i\omega_n) \times \sum_{\omega_2,\omega_l} \mathcal{A}_{\bar{\sigma}}(i\omega_l) g_{0\sigma}(i\omega_2) I(\omega_n,\omega_l,\omega_2), \quad (22)$$

with

$$I(\omega_n,\omega_l,\omega_2) \equiv \int_0^\beta d\tau_2 e^{i(\omega_l-\omega_2)\tau_2} \int_0^{\tau_2} d\tau_1 e^{i(\omega_n-\omega_l)\tau_1}. \quad (23)$$

In order to evaluate I, we can consider five cases:
(A) $\omega_2 = \omega_l = \omega_n$,
(B) $\omega_2 = \omega_n \neq \omega_l$,
(C) $\omega_2 = \omega_l \neq \omega_n$,
(D) $\omega_2 \neq \omega_l = \omega_n$,
(E) $\omega_2 \neq \omega_l$ and $\omega_l \neq \omega_n$.

In case (A) both exponents in the integrand of Eq. (23) vanish, and we have

$$I^{(A)} = \int_0^\beta d\tau_1 \int_0^{\tau_1} d\tau_2 = \beta^2/2. \quad (24)$$

This gives the first contribution

$$\Lambda_1^{(A)}(i\omega_n) = \frac{1}{2} g_{0\sigma}(i\omega_n)\mathcal{A}_{\bar{\sigma}}(i\omega_n) g_{0\sigma}(i\omega_n). \quad (25)$$

It is easy to show that for the next two cases, the results are

$$\Lambda_1^{(B)}(i\omega_n) = -g_{0\sigma}(i\omega_n)\frac{1}{\beta}\sum_{\nu_l\neq 0} \frac{\mathcal{A}_{\bar{\sigma}}(i\omega_n+i\nu_l)}{i\nu_l} g_{0\sigma}(i\omega_n) \quad (26)$$

and

$$\Lambda_1^{(C)}(i\omega_n) = g_{0\sigma}(i\omega_n)\frac{1}{\beta}\sum_{\nu_l\neq 0} \frac{\mathcal{A}_{\bar{\sigma}}(i\omega_n+i\nu_l) g_{0\sigma}(i\omega_n+i\nu_l)}{i\nu_l}, \quad (27)$$

while $\Lambda_1^{(D)} = \Lambda_1^{(E)} = 0$. In Fig. 3, we show the on-site diagrammatic representation of Λ_1 when one uses only contractions, introducing the bosonic Green's functions that appear

as wavy lines in the diagrams.[15] Those diagrams can be viewed as representing Eqs. (26) and (27), if the factors $1/i\nu_l$ appearing in these equations are associated with the bosonic Green's functions. Thus, with the above procedure we have managed to separate the contribution corresponding to $\nu_l=0$, obtaining a finite limit for this term. An equivalent development can be made for all the other terms, similar in form to Γ_1, that result from the Hubbard operator representation of the electron operators appearing in Eq. (16).

C. Simple approximation

We now turn to a simplified treatment of the corrections due to spin fluctuations that can be viewed as a kind of *static approximation*. It consists of neglecting all terms that involve nonzero bosonic frequencies in the corrections to the local irreducible Green's function. In the example developed above, we take only the term $\Lambda_1^{(A)}$. We see then that the new terms are similar in form to those that we had when only equal spin contributions were considered, except for the fact that the local effective field is that associated with electrons of opposite spin. Another important difference is that there can be mixed terms involving both $g_{0\sigma}$ and $g_{\bar{\sigma}\bar{2}}$, since the contractions that generate bosonic operators do *not* generate the projectors n_σ or $1-n_\sigma$.

Restricting the analysis to the half-filling case, corrections coming from terms that contain a bosonic operator of the kind X_{02} present the same structure as obtained for $X_{\bar{\sigma}\sigma}$, except for an overall change of sign together with a change of sign of the frequency argument of the local effective field. Hence, they just double the terms coming from averages involving $X_{\bar{\sigma}\sigma}$ since at half filling the equality $\mathcal{A}_\sigma(-i\omega_n)=-\mathcal{A}_\sigma(i\omega_n)$ is verified. The total change of $G_{ii\sigma}$, with respect to the FK result to the first order in $\mathcal{A}_{\bar{\sigma}}$ is

$$\Delta G_{ii\sigma}=(g_{0\sigma}-g_{\bar{\sigma}\bar{2}})\mathcal{A}_{\bar{\sigma}}[\langle 1-n_{\bar{\sigma}}\rangle g_{0\sigma}-\langle n_{\bar{\sigma}}\rangle g_{\bar{\sigma}\bar{2}}], \quad (28)$$

where we left implicit the frequency dependence, which is the same for all the Green's functions and the effective field $\mathcal{A}$.

When we go to higher orders, the *effective structure* of the diagrams in the static approximation is the same as in the FK model, shown in Fig. 2, except that effective-field lines can refer to both spin orientations. The series is summable, and the single-site Green's function, including the opposite-spin contributions in the static approximation, can be written in the form

$$G_{ii\sigma}(i\omega_n)=\frac{1-\langle n_{\bar{\sigma}}\rangle}{i\omega_n+\mu-\mathcal{A}_\sigma(i\omega_n)}[1+\alpha_1(i\omega_n)] + \frac{\langle n_\downarrow\rangle}{i\omega_n+\mu-U-\mathcal{A}_\sigma(i\omega_n)}[1+\alpha_2(i\omega_n)], \quad (29)$$

where

$$\alpha_1\equiv\frac{(g_{0\sigma}-g_{\bar{\sigma}\bar{2}})\mathcal{A}_{\bar{\sigma}}}{1-\mathcal{A}_\sigma g_{0\sigma}-\mathcal{A}_{\bar{\sigma}}(g_{0\sigma}+g_{\bar{\sigma}\bar{2}})} \quad (30)$$

and

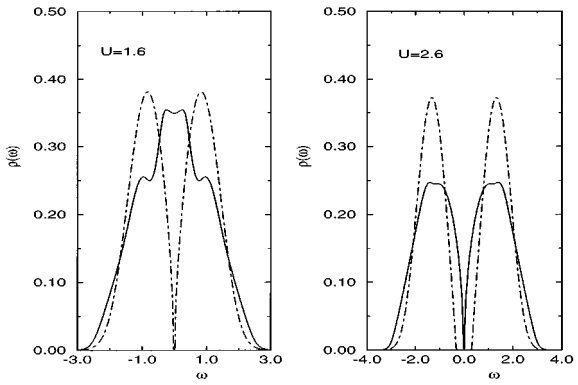

FIG. 4. Densities of states in the half-filled paramagnetic state for the FK model (dashed) and for our simple approximation to the Hubbard model (continuous). The results are shown for two values of U (see text for details). All energies are measured in units of t^*.

$$\alpha_2\equiv\frac{(g_{\bar{\sigma}\bar{2}}-g_{0\sigma})\mathcal{A}_{\bar{\sigma}}}{1-\mathcal{A}_\sigma g_{\bar{\sigma}\bar{2}}-\mathcal{A}_{\bar{\sigma}}(g_{0\sigma}+g_{\bar{\sigma}\bar{2}})}. \quad (31)$$

Notice that the corrections to the FK Green's function vanish for $\mathcal{A}_{\bar{\sigma}}=0$ (by construction), and also for $U=0$ (since in this case $g_{\bar{\sigma}\bar{2}}=g_{0\sigma}$), which is consistent with the fact that the two spin species become independent in the noninteracting limit.

After analytically continuing $G_{ii\sigma}(i\omega_n)\rightarrow G_{ii\sigma}(z)$, for an arbitrary complex frequency z, we can consider the retarded case $z=\omega+i0^+$, for real ω, and calculate the single-particle DOS. Results for the paramagnetic state are shown in Fig. 4, in comparison with the corresponding ones for the FK model. We have chosen two values of U close to the critical values for a metal-insulator transition for each solution. We see that the transition occurs in the FK model for a substantially lower value of U, with respect to the Hubbard model in the approximation that we are using. Nevertheless, the critical U obtained here for the Hubbard model is still low in comparison with numerical calculations.[7,11] One interesting feature noticeable in Fig. 4 is the presence of a central peak in the DOS for the Hubbard case in the small-U limit, which never happens for the FK solution. However, despite the presence of a central peak, this approximation does not recover a Fermi-liquid state, except strictly at $U=0$. Indeed, one can see in Fig. 4 that the central peak presents some structure: a shallow dip in the middle, which becomes more pronounced, although narrower, as U is further reduced. For very large U the Hubbard and FK solutions are essentially coincident.

V. THE ANTIFERROMAGNETIC STATE

Up to now our analysis of the Hubbard model (or its simplified form, the FK model) has been restricted to the paramagnetic phase. However, this phase is not expected to be stable for $n=1$ in the limit of strong Coulomb interaction, or even for arbitrary interaction strength in the case of hypercubic lattices with nearest-neighbor hopping. In the large-U limit it is well known[22] that the Hubbard model reduces to the AF Heisenberg model, with an effective exchange inter-

action $J=t^2/U$. In the weak coupling regime, one also expects an ordered state, although of a different nature: it is driven by an instability of the paramagnetic state against the formation of a spin-density wave of wave vector $\mathbf{Q}=(\pi,\pi,\pi,\ldots)$. This is due to the nesting property of the Fermi surface corresponding to a half-filled tight-binding band in a hypercubic lattice with nearest-neighbor hopping only.

In the search for an ordered phase of the half-filled Hubbard model, and still addressing the infinite dimension limit, we will use a similar approach as for the paramagnetic case, starting with the exact solution of the FK model, and adding corrections due to the mobility of the other spin species within the approximation introduced in the previous section. The ordered phase of the FK model was studied by Brandt and Mielsch.[23] This phase is not exactly an antiferromagnetically ordered state, but rather a *checkerboard* arrangement of the nonmobile electrons, with the mobile ones occupying preferably the other sublattice at low temperatures. However, the asymmetry between the mobilities of the two spin species yields an asymmetry in sublattice occupation, and the sublattice magnetization does not saturate. Brandt and Mielsch have chosen as order parameter the occupation number of nonmobile electrons in the sublattice that they populate at low temperature. Then, the critical temperature (T_c) is that for which this occupation number comes down to 1/2. Obviously, T_c depends on the strength of the interaction, which allows for the construction of a phase-diagram $T_c \times U$.

In order to treat the AF state in the Hubbard model or the checkerboard phase of the FK model, we divide the lattice in two sublattices, A and B. Since we are dealing with a bipartite lattice with nearest-neighbor hopping, the self-consistency condition fulfilled by the single-site Green's functions for electrons of spin σ (to be considered as the mobile ones in the case of the FK model) reads

$$G^{\alpha}_{ii\sigma}(i\omega_n)=\frac{\overline{\xi_\sigma}}{\xi^{\alpha}_{\sigma}}F(\overline{\xi_\sigma}), \tag{32}$$

where $F(x)$ is defined in Eq. (11), α ($=A$ or B) labels the sublattice,

$$\xi^{\alpha}_{\sigma}=1/G^{\alpha}_{ii\sigma}+\mathcal{A}^{\alpha}_{\sigma}, \tag{33}$$

and $\overline{\xi_\sigma}\equiv\sqrt{\xi^A_\sigma \xi^B_\sigma}$. The form of the Green's function is given by Eqs. (15) or (29), depending on the model studied. The completely self-consistent solution requires an evaluation of the average number of electrons with each spin orientation per site, which is achieved, in principle, by summing the respective Green's function over Matsubara's frequency. In the FK model though the nonmobile electron Green's function is difficult to calculate, and their number is determined directly from the partition function, which is exactly known. The resulting relation is[23]

$$\langle n^{\alpha}_{\sigma}\rangle=\left\{1+\exp\sum_n\ [\ln(i\omega_n+U/2-\mathcal{A}^{\alpha}_{\sigma}) - \ln(i\omega_n-U/2-\mathcal{A}^{\alpha}_{\sigma})]e^{i\omega_n 0^+}\right\}^{-1}, \tag{34}$$

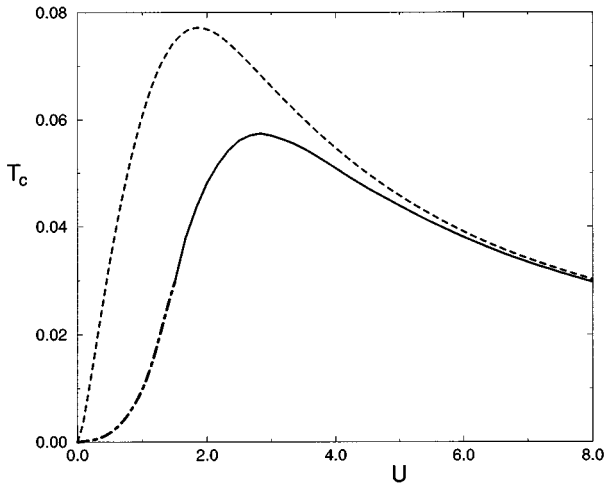

FIG. 5. Phase diagram showing the variation of the ordering transition temperature T_c, with the interaction strength U for both the FK (dashed) and Hubbard (continuous) models. The dot-dashed line denotes the region where the results of the approximation considered for the Hubbard model are not reliable, due to numerical problems.

where we have explicitly used the value of the chemical potential at half filling, $\mu=U/2$.

For the Hubbard model, the Green's functions associated with electrons of both spin orientations are equivalent in form, and the determination of both occupation numbers by the sum of the corresponding Green's functions should give the correct results. However, if we take this approach with the approximation that we are employing here, we *do not* find an AF solution for any value of the interaction. To understand this we have to remember that our approximation starts with the exact Green's function of the FK model for a given spin orientation, and adds corrections due to the mobility of the opposite-spin electrons. Since these corrections are only included in an approximate form, the full spin symmetry of the Hubbard model is not recovered. A more consistent approach would be then to look at the changes in the two (nonsymmetrical) sublattice magnetizations introduced by this partial dynamics of the previously nonmobile electrons. The problem now is that we no longer have an exact partition function from which we could determine $\langle n^{\alpha}_{\sigma}\rangle$. We will then look for a relation equivalent to Eq. (34) by comparing the structure of the exact solution of the FK model and that of the approximate one for the Hubbard case. First we notice that Eq. (34) can be rewritten in the form

$$\langle n^{\alpha}_{\sigma}\rangle=\left\{1+\exp\sum_n\ [\ln\widetilde{g}^{\ -1}_{0\sigma}(i\omega_n)-\ln\widetilde{g}^{\ -1}_{\overline{\sigma 2}}(i\omega_n)]e^{i\omega_n 0^+}\right\}^{-1}, \tag{35}$$

where $\widetilde{g}_{0\sigma}(i\omega_n)$ and $\widetilde{g}_{\overline{\sigma 2}}(i\omega_n)$ are nothing but the atomic Green's functions $g_{0\sigma}(i\omega_n)$ and $g_{\overline{\sigma 2}}(i\omega_n)$ renormalized by the presence of the effective field $\mathcal{A}$. From Eq. (29), we can see that these Green's functions are further renormalized by factors coming from the inclusion of the dynamics of the electrons with spin $\overline{\sigma}$. If we keep the form of Eq. (35), but include the extra renormalization, we do obtain an ordered solution. The phase diagram is shown in Fig. 5, in compari-

son with the one for the FK model. The part represented by a dot-dashed line is somewhat ''guessed'' to match the exact point at the origin, because we have problems of convergence of the self-consistency process in this region of the phase diagram. This is consistent with the fact that this approximation becomes worse in the region of weak interaction, as we already noted in connection to the DOS.

We remark on the fact that the phase diagram obtained from the approximate solution of the Hubbard model differs from the results of numerical solutions[7,12] in a fundamental way: here, the FK solution appears as an upper limit for the Hubbard one, i.e., critical temperatures are smaller in the Hubbard case for equal values of U, while the opposite is verified in quantum Monte Carlo calculations. Presently, we do not know the origin of this discrepancy. In principle, one would be tempted to conclude that our approximation is too crude to give even qualitatively reliable results. However, considering that we started from the exact solution of the FK model, it seems likely that the mobility of the previously frozen electrons should help in unstabilizing the ordered state. If this is true, the transition temperatures for the FK model should indeed be an upper limit for those of the Hubbard case.

VI. CONCLUSIONS

We have studied the infinite dimension limit of the Hubbard model and its simplified version, the Falicov-Kimball model, by means of perturbation theory around the atomic limit. This method provides a simple way of rederiving the exact mapping of the model to a single-site problem, in the presence of an effective field and subject to a self-consistency condition that relates it to the lattice problem. Furthermore, the method provides an alternative approach for studying this single-site problem by means of a perturbation series in the effective local field. We have shown that this series is exactly summable for the FK model, reproducing results previously obtained by Brandt and Mielsch.[4,23] Based on this, we proposed an approach to the study of the full Hubbard model in $d=\infty$: it consists in starting with the exact Green's function of the FK model for electrons with a given spin orientation, and adding corrections due to the dynamics of the opposite-spin electrons. Since the problem is not exactly solvable, some approximation must be worked out in extracting these corrections from the formal series in the effective field.

We have exemplified this method here with a simple approximation that keeps only the static (zero frequency) contribution from atomic excitations involving spin-flip or charge-pair fluctuations. In what refers to the single-particle DOS in the paramagnetic phase, our approximate solution gives the correct large-U limit, but fails in the weak-coupling regime. Nevertheless, this failure is not dramatic, since the qualitatively expected structure of the DOS is observed: a central peak, and the two satellite precursors of the Hubbard subbands. The failure resides in the detailed shape of the central peak, and the fact that it is not pinned to the noninteracting DOS at the Fermi level. This is a signature of a breakdown of the Fermi-liquid state for any nonzero U, which is consistent with the fact that the spin symmetry of the Hubbard model is not fully recovered in this simple approximation. This asymmetry is clearly seen in the fact that the ''antiferromagnetic'' phase is qualitatively similar to the checkerboard phase of the FK model. From the comparison between phase diagrams for the two models, we raised the interesting question of whether or not the critical temperatures for the FK model should provide an upper limit to those of the Hubbard one for equal interaction strength, as obtained here in contrast to quantum Monte Carlo results.

Despite the deficiencies of the approximation that we have discussed, we believe that the method outlined above can be an interesting alternative or complement to weak-coupling approaches to the infinite dimensional Hubbard model, as far as analytical methods are concerned. In our opinion, the main point to be explored in the future is a better way of dealing with the intravertex diagrammatics. There is some room for choice in applying the generalized Wick's theorem for Hubbard operators. Different priority rules lead to different diagrammatic structures, and better suited schemes may be expected to show up in future explorations of this issue.

ACKNOWLEDGMENTS

We acknowledge support by the Brazilian agencies Conselho Nacional de Desenvolvimento Científico e Tecnológico (CNPq), Financiadora de Estudos e Projetos (FINEP), and Fundação de Amparo à Pesquisa do Estado do Rio Grande do Sul (FAPERGS).

*Permanent address: Instituto de Física, Universidade Federal do Rio Grande do Sul, 91501-970 Porto Alegre, RS, Brazil.

[1] W. Metzner and D. Vollhardt, Phys. Rev. Lett. **62**, 324 (1989); E. Müller-Hartmann, Z. Phys. B **74**, 507 (1989). For a review see D. Vollhardt, in *Correlated Electron Systems*, Proceedings of the Jerusalem Winter School of Theoretical Physics, edited by V. J. Emery (World Scientific, Singapore, 1993).

[2] J. Hubbard, Proc. R. Soc. London Ser. A **276**, 238 (1963).

[3] A. Georges and G. Kotliar, Phys. Rev. B **45**, 6479 (1992).

[4] U. Brandt and C. Mielsch, Z. Phys. B **75**, 365 (1989).

[5] P. G. J. van Dongen and D. Vollhardt, Phys. Rev. Lett. **65**, 1663 (1990); V. Janis, Z. Phys. B **83**, 227 (1991); V. Janis and D. Vollhardt, *ibid.* **91**, 317 (1993).

[6] L. M. Falicov and J. C. Kimball, Phys. Rev. Lett. **22**, 997 (1969).

[7] M. Jarrel, Phys. Rev. Lett. **69**, 168 (1992).

[8] A. Georges and W. Krauth, Phys. Rev. Lett. **69**, 1240 (1992).

[9] M. J. Rozenberg, X. Y. Zhang, and G. Kotliar, Phys. Rev. Lett. **69**, 1236 (1992).

[10] M. Caffarel and W. Krauth, Phys. Rev. Lett. **72**, 1545 (1994).

[11] X. Y. Zhang, M. J. Rozenberg, and G. Kotliar, Phys. Rev. Lett. **70**, 1666 (1993).

[12] A. Georges and W. Krauth, Phys. Rev. B **48**, 7167 (1993).

[13] Generalization to the Bethe lattice is straightforward.

[14] W. Metzner, Phys. Rev. B **43**, 8549 (1991).

[15] L. Craco and M. A. Gusmão, Phys. Rev. B **52**, 17 135 (1995).

[16] J. Hubbard, Proc. R. Soc. London Ser. A **277**, 237 (1964).

[17] E. Anda, J. Phys. C **14**, L1037 (1981).

[18] A. A. Abrikosov, L. P. Gorkov, and I. E. Dzyaloshinski, *Methods of Quantum Field Theory in Statistical Physics* (Prentice-Hall, Englewood Cliffs, NJ, 1963).

[19] J. Hubbard, Proc. R. Soc. London Sect. A **281**, 401 (1964).

[20] In our approach the self-energy is $\Sigma_\sigma(i\omega_n) \equiv i\omega_n + \mu - \mathcal{G}_\sigma^{-1}(i\omega_n)$.

[21] Other priority rules lead to different diagrammatic representations. See, for example, M. Bartkowiak and K. A. Chao, Phys. Rev. B **47**, 4193 (1993).

[22] P. W. Anderson, in *Solid State Physics: Advances in Research and Applications*, edited by F. Seitz and D. Turnbull (Academic, New York, 1963), Vol. 14, p. 99.

[23] U. Brandt and C. Mielsch, Z. Phys. B **79**, 295 (1990).